Unsplit-field PML formulation for shallow-water equations and finite volume method

Chaiwoot Boonyasiriwat

ABSTRACT

This report presents the 6-month research progress on the project titled "Development of parallel programs for tsunami simulation" funded by IPST under the grant number 001/2558. The progress is composed of two parts. In the first part, an unsplit-field PML formulation for the shallow-water equations was derived to modeling tsunami wave propagation in unbounded domains. In the second part, the theory of finite volume method which is a method of choice for solving nonlinear hyperbolic systems are presented with a numerical experiment on the 1D linear advection equation.

INTRODUCTION

Perfectly matched layer (PML) is the most widely used method for modeling wave propagation in unbounded domains due to its effectiveness and efficiency compared to other methods. The original version of PML developed by Bérenger (1994) now known as a split-field PML formulation for the Maxwell's equations was shown to be unstable by Abarbanel and Gottlieb (1997). The split-field PML method was later applied to linearized Euler equations by Hu (1996). Similarly to the case of Maxwell's equations, the split-field PML formulation for linearized Euler equations was also shown to be unstable by Hesthaven (1998). Stable PML formulations were later presented in the so-called unsplit-field form for Maxwell's equations (Abarbanel and Gottlieb, 1998) and linearized Euler equations (Hesthaven, 1998; Abarbanel et al., 1999; Hu, 2001). The split-field PML of Bérenger (1994) was later applied to linearized shallow-water equations by Navon et al. (2004) and, as expected, the resulting PML equations are unstable and a filter was needed to obtain a stable result. Abarbanel et al. (2003) applied the approach of Abarbanel et al. (1999) and Hu (2001) and obtained two unsplit-field PML formulations stable for the linearized shallow-water equations but unstable for the nonlinear case. Recently, Barucq et al. (2010) applied the approach of Nataf (2006) to derive a stable PML formulation for linearized shallow-water equations. Stable PML formulation for nonlinear shallow-water equations is still an open problem.

In this report, I present unsplit-field PML formulations in primitive variables for 1D and 2D shallow-water equations. The derivation of the PML equations for the 1D case is first presented. Then the same procedure was applied to obtain the 2D formulation which are given without a derivation. To compare the effectiveness and stability of the proposed PML formulation, I need to learn the finite volume method which is currently one of the most widely used methods for solving nonlinear systems of conservation laws including the shallow-water equations. The finite volume method can accurately recover discontinuous solutions or shock waves and, therefore, it is suitable for tsunami simulation which include shock-wave solutions near the coastline. The second part of this report presents the result of my learning of the finite volume method which is given in the form of concise theory and preliminary numerical experiment.

PML FORMULATIONS FOR SHALLOW-WATER EQUATIONS

1D Shallow-Water Equations

In this section, we present the derivation of an unsplit-field PML formulation for the 1D shallow-water equations given as

$$\begin{aligned} h_{,t} + uh_{,x} + hu_{,x} &= 0, \\ u_{,t} + uu_{,x} + gh_{,x} &= 0, \end{aligned} \tag{1}$$

where $a_{,b} \equiv \partial a/\partial b$, h is wave height, u is depth-averaged particle velocity in x-direction, g is gravitational acceleration.

Applying temporal Fourier transform to equations 1 yields

$$\begin{aligned} -i\omega\tilde{h} + \tilde{u} * \tilde{h}_{,x} + \tilde{h} * \tilde{u}_{,x} &= 0, \\ -i\omega\tilde{u} + \tilde{u} * \tilde{u}_{,x} + g\tilde{h}_{,x} &= 0, \end{aligned} \tag{2}$$

where $*$ denotes temporal convolution and $\tilde{\square}$ is the temporal Fourier transform of $\square$. Using the coordinate stretching approach of Chew and Weedon (1994), the spatial derivatives in equation 2 is replaced by

$$\frac{\partial}{\partial x} \rightarrow \left(\frac{1}{1 + \frac{i\sigma(x)}{\omega}} \right) \frac{\partial}{\partial x} = \alpha(x) \frac{\partial}{\partial x} \tag{3}$$

where $\sigma(x) > 0$ in the PML region and $\sigma(x) = 0$ in the physical region, and we then obtain the PML equations in the frequency domain, namely,

$$\begin{aligned} -i\omega\tilde{h} + \tilde{u} * (\alpha\tilde{h}_{,x}) + \tilde{h} * (\alpha\tilde{u}_{,x}) &= 0, \\ -i\omega\tilde{u} + \tilde{u} * (\alpha\tilde{u}_{,x}) + g(\alpha\tilde{h}_{,x}) &= 0, \end{aligned} \tag{4}$$

Using the two auxiliary variables $\tilde{H}_x$ and $\tilde{U}_x$ defined as

$$\begin{aligned} -i\omega\tilde{H}_x &= \alpha\tilde{h}_{,x}, \\ -i\omega\tilde{U}_x &= \alpha\tilde{u}_{,x}, \end{aligned} \tag{5}$$

equation 4 becomes

$$\begin{aligned} -i\omega\tilde{h} + \tilde{u} * (-i\omega\tilde{H_x}) + \tilde{h} * (-i\omega\tilde{U_x}) = 0, \\ -i\omega\tilde{u} + \tilde{u} * (-i\omega\tilde{U_x}) + g(-i\omega\tilde{H_x}) = 0, \end{aligned} \tag{6}$$

Applying inverse Fourier transform to equations 5 and 6 yields

$$\begin{aligned} h_{,t} + uH_{x,t} + hU_{x,t} = 0 \\ u_{,t} + uU_{x,t} + gH_{x,t} = 0 \end{aligned} \tag{7}$$

Equation 5 can be rewritten as

$$\begin{aligned} (-i\omega + \sigma)\,\tilde{H_x} = \tilde{h}_{,x}, \\ (-i\omega + \sigma)\,\tilde{U_x} = \tilde{u}_{,x}, \end{aligned} \tag{8}$$

Applying inverse Fourier transform to equations 8 yields

$$\begin{aligned} H_{x,t} + \sigma H_x = h_{,x} \\ U_{x,t} + \sigma U_x = u_{,x} \end{aligned} \tag{9}$$

Using equation 9, equation 7 can be rewritten as

$$\begin{aligned} h_{,t} + u(h_{,x} - \sigma H_x) + h(u_{,x} - \sigma U_x) = 0 \\ u_{,t} + u(u_{,x} - \sigma U_x) + g(h_{,x} - \sigma H_x) = 0 \end{aligned} \tag{10}$$

Equations 9 and 10 constitute the unsplit-field PML formulation in primitive variables for the 1D shallow-water equation 1.

2D Shallow-Water Equations

In this section, we apply the same procedure given in the previous section to the 2D shallow-water equations given as

$$\begin{aligned} h_{,t} + uh_{,x} + vh_{,y} + h(u_{,x} + v_{,y}) = 0, \\ u_{,t} + uu_{,x} + vu_{,y} + gh_{,x} - fv = 0, \\ v_{,t} + uv_{,x} + vv_{,y} + gh_{,y} + fu = 0, \end{aligned} \tag{11}$$

where u and v are the particle velocity in x- and y-directions, respectively, and f is the Coriolis factor, and obtain the unsplit-field PML equations in primitive variables as follows.

$$\begin{aligned} h_{,t} + u(h_{,x} - \sigma_x H_x) + v(h_{,y} - \sigma_y H_y) \\ +h(u_{,x} - \sigma_x u_x + v_{,y} - \sigma_y v_y) = 0, \\ u_{,t} + u(u_{,x} - \sigma_x U_x) + v(u_{,y} - \sigma_y U_y) \\ +g(h_{,x} - \sigma_x H_x) - fv = 0, \\ v_{,t} + u(v_{,x} - \sigma_x V_x) + v(v_{,y} - \sigma_y V_y) \\ +g(h_{,y} - \sigma_y H_y) + fu = 0, \\ H_{x,t} + \sigma_x H_x = h_{,x} \\ H_{y,t} + \sigma_y H_y = h_{,y} \\ U_{x,t} + \sigma_x U_x = u_{,x} \\ U_{y,t} + \sigma_y U_y = u_{,y} \\ V_{x,t} + \sigma_x V_x = v_{,x} \\ V_{y,t} + \sigma_y V_y = v_{,y} \end{aligned} \tag{12}$$

where $H_x, H_y, U_x, U_y, V_x, V_y$ are auxiliary variables, and σ_x and σ_y are the absorption coefficient in x- and y-directions, respectively.

FINITE VOLUME METHOD

In this section, I present the theory of finite volume method which is suitable for numerically solving nonlinear systems of conservation laws. So I begin with the introduction to conservation laws. Then I explain the finite volume method.

Scalar Conservation Laws

A scalar conservation law in one space dimension can be expressed in the integral form as

$$\frac{d}{dt}\int_{x_1}^{x_2} q(x,t)dx = f(q,x_1,t) - f(q,x_2,t), \tag{13}$$

where $q(x,t)$ is the conserved quantity and $f(q,x,t)$ is a flux function. In most cases, we will be dealing with autonomous flux $f(q)$ which does not depend explicitly on x and t. Equation 13 then becomes

$$\frac{d}{dt}\int_{x_1}^{x_2} q(x,t)dx = f(q(x_1,t)) - f(q(x_2,t)). \tag{14}$$

It can be shown that equation 14 can be rewritten as (LeVeque, 2002)

$$\int_{x_1}^{x_2}\left[\frac{\partial q(x,t)}{\partial t} + \frac{\partial f(q(x,t))}{\partial x}\right]dx = 0. \tag{15}$$

Equation 15 implies that the integrand must vanish and leads to the differential form of the conservation law, namely

$$\frac{\partial q(x,t)}{\partial t} + \frac{\partial f(q(x,t))}{\partial x} = 0, \tag{16}$$

which is called the conservative form. Equation 16 can also be written in the quasilinear form as

$$\frac{\partial q(x,t)}{\partial t} + \frac{df}{dq}\frac{\partial q(x,t)}{\partial x} = 0. \tag{17}$$

Method of Characteristics

A characteristic curve along which q is constant can be determined by setting the total derivative of $q(x,t)$ to zero, i.e., The total derivative of $q(x,t)$ is

$$\frac{dq}{dt} = \frac{\partial q}{\partial t} + \frac{dx}{dt}\frac{\partial q}{\partial x} = 0. \tag{18}$$

Comparing equations 17 and 18, we obtain the relation

$$\frac{dx}{dt} = \frac{df}{dq} \tag{19}$$

whose solution is the characteristic curve

$$x = x_0 + \frac{df}{dq}t, \tag{20}$$

where x_0 is a constant of integration.

Linear Advection Equation

Consider the Cauchy problem for the 1D linear advection equation given by

$$\begin{aligned} \frac{\partial q}{\partial t} + u\frac{\partial q}{\partial x} &= 0, \\ q(x,0) &= \tilde{q}(x), \qquad x \in \Re \end{aligned} \tag{21}$$

where the fluid velocity u is constant and $\tilde{q}$ is some function. In this case, the flux function is $f(q) = uq$ and the characteristic curve satisfies

$$\frac{dx}{dt} = \frac{df}{dq} = u, \tag{22}$$

so the curve itself is given by

$$x(t) = x_0 + ut. \tag{23}$$

Since q is constant along the characteristics, we can express the solution to the Cauchy problem 21 as

$$q(x,t) = \tilde{q}(x - ut). \tag{24}$$

Inviscid Burgers Equation

The inviscid Burgers equation given by

$$\frac{\partial u}{\partial t} + \frac{\partial}{\partial x}\left(\frac{1}{2}u^2\right) = \frac{\partial u}{\partial t} + u\frac{\partial u}{\partial x} = 0 \tag{25}$$

models the conservation of momentum ρu of an inviscid and incompressible fluid with no pressure gradient. Since the mass density ρ is constant, it was removed from the momentum equation resulting in the conservation of the fluid velocity u.

Consider again the Cauchy problem with initial data given by

$$u(x,0) = \tilde{u}(x), \qquad x \in \Re \tag{26}$$

In this case, the characteristics also satisfy

$$\frac{dx}{dt} = u. \tag{27}$$

So a solution to the Cauchy problem 26 for the inviscid Burgers equation 25 is

$$u(x,t) = \tilde{u}(x - ut). \tag{28}$$

Note that this is an implicit equation for the solution since the solution itself appears as the argument of the initial condition on the right-hand side. The exact solution of the inviscid Burgers equation can be obtained using the Cole-Hopf transformation (LeVeque, 2002).

Although the characteristic equation of the Burgers equation has the same form as that of the linear advection equation, all the characteristic curves of the linear advection equation have the same slope and will never collide while the characteristic curves of the Burgers equation can have different slopes depending on the initial function $\tilde{u}$. When the characteristic curves collide, a shock wave is formed even when the initial function is smooth.

Advective Acoustics Equations

When the perturbation is small, the Euler equations can be linearized into the advective acoustics equations

$$q_{,t} + Aq_{,x} = 0, \tag{29}$$

where

$$q(x,t) = \begin{bmatrix} p(x,t) \\ u(x,t) \end{bmatrix} \tag{30}$$

is the perturbation from the fixed state

$$q_0 = \begin{bmatrix} p_0 \\ u_0 \end{bmatrix} \tag{31}$$

and

$$A = \begin{bmatrix} u_0 & K_0 \\ 1/\rho_0 & u_0 \end{bmatrix}. \tag{32}$$

Here K is the bulk modulus, ρ is mass density, p is pressure, and u_0 is fluid particle velocity.

The matrix A has the eigenvalues

$$\begin{aligned} \lambda_1 &= u_0 - c_0, \\ \lambda_2 &= u_0 + c_0, \end{aligned} \tag{33}$$

and the corresponding normalized eigenvectors

$$\begin{aligned} r_1 &= \begin{bmatrix} -Z_0/\sqrt{1+Z_0^2} \\ 1/\sqrt{1+Z_0^2} \end{bmatrix} \\ r_2 &= \begin{bmatrix} Z_0/\sqrt{1+Z_0^2} \\ 1/\sqrt{1+Z_0^2} \end{bmatrix} \end{aligned} \tag{34}$$

where the sound speed $c_0 = \sqrt{K_0/\rho_0}$ and the impedance $Z_0 = \rho_0 c_0$.

Shallow Water Equations

The one-dimensional shallow water equations can be written in the conservation form as

$$q_{,t} + f(q)_{,x} = 0, \tag{35}$$

where the conserved quantity q is

$$q(x,t) = \begin{bmatrix} h \\ hu \end{bmatrix}, \tag{36}$$

and the flux function f is

$$f(x,t) = \begin{bmatrix} uh \\ hu^2 + \frac{1}{2}gh^2 \end{bmatrix}. \tag{37}$$

Here h is the wave height or fluid depth, u is the particle velocity, and g is the gravitational acceleration.

To use the finite-volume method, we need to turn the shallow-water equations into the quasilinear form, given by

$$q_{,t} + f'(q)q_{,x} = 0, \tag{38}$$

where the Jacobian matrix $f'(q)$ is

$$f'(q) = \begin{bmatrix} 0 & 1 \\ -u^2 + gh & 2u \end{bmatrix}. \tag{39}$$

The eigenvalues of $f'(q)$ are

$$\begin{aligned} \lambda^1 &= u - \sqrt{gh}, \\ \lambda^2 &= u + \sqrt{gh}, \end{aligned} \tag{40}$$

and the corresponding eigenvectors are

$$\begin{aligned} r^1 &= \begin{bmatrix} 1 \\ u - \sqrt{gh} \end{bmatrix}, \\ r^2 &= \begin{bmatrix} 1 \\ u + \sqrt{gh} \end{bmatrix}. \end{aligned} \tag{41}$$

Conservative Numerical Schemes

In finite volume method, the spatial domain is discretized into a finite number of cells or finite volumes. In 1D, the ith cell is denoted by

$$C_i = (x_{i-1/2}, x_{i+1/2}). \tag{42}$$

The integral form of the conservation law 14 for the ith cell is given by

$$\frac{d}{dt}\int_{C_i} q(x,t)dx = f(q(x_{i-1/2},t)) - f(q(x_{i+1/2},t)). \tag{43}$$

Integrating equation 43 in time from t_n to t_{n+1} and rearranging the resulting equation, we obtain

$$Q_i^{n+1} = Q_i^n - \frac{\Delta t}{\Delta x}(F_{i+1/2}^n - F_{i-1/2}^n), \tag{44}$$

where the cell average Q_i^n and the numerical flux $F_{i-1/2}^n$ are defined as

$$\begin{aligned} Q_i^n &\approx \frac{1}{\Delta x}\int_{C_i} q(x,t_n)dx, \\ F_{i-1/2}^n &\approx \frac{1}{\Delta t}\int_{t_n}^{t_{n+1}} f(q(x_{i-1/2},t))dt. \end{aligned} \tag{45}$$

Here, $\Delta x = x_{i+1/2} - x_{i-1/2}$ and $\Delta t = t_{n+1} - t_n$. Any numerical scheme that can be written in the form 44 are said to be a conservative scheme (LeVeque, 2002).

Lax-Friedrichs Scheme

The Lax-Friedrichs (LxF) scheme for a scalar conservation law is given by

$$Q_i^{n+1} = \frac{1}{2}(Q_{i-1}^n + Q_{i+1}^n) - \frac{\Delta t}{2\Delta x}\left[f(Q_{i+1}^n) - f(Q_{i-1}^n)\right], \tag{46}$$

When written in the form of conservative scheme 44, the numerical flux of the LxF scheme is

$$F_{i-1/2}^n = \frac{1}{2}\left[f(Q_{i-1}^n) + f(Q_i^n)\right] - \frac{\Delta x}{2\Delta t}(Q_i^n - Q_{i-1}^n), \tag{47}$$

The LxF scheme is first-order accurate in both time and space, and can be applied to both linear and nonlinear scalar hyperbolic problems.

First-Order Upwind Scheme

An upwind scheme uses the flow direction to determine how to approximate the spatial derivative terms. Let's use the linear advection equation 21 as an example. When $u > 0$, the conserved quantity q is advected from left to right so the spatial derivative $q_{,x}$ is approximated as

$$q_{,x} \approx \frac{q(x_i,t) - q(x_{i-1},t)}{\Delta x}. \tag{48}$$

Using this approximation, the linear advection equation becomes the semi-discrete scheme

$$\frac{dq_i(t)}{dt} + u\frac{q_i(t) - q_{i-1}(t)}{\Delta x} = 0, \tag{49}$$

where $q_i(t) = q(x_i,t)$. If the forward Euler method is used, we obtain the fully discrete scheme

$$q_i^{n+1} = q_i^n - \frac{u\Delta t}{\Delta x}(q_i^n - q_{i-1}^n). \tag{50}$$

Note that this is an upwind finite-difference scheme which becomes an upwind finite-volume scheme if q_i^n is thought of as the cell average Q_i^n.

Riemann Problem

The Riemann problem is composed of a hyperbolic PDE and an initial condition in the form of a piecewise-constant function with a discontinuity,

$$q_0(x) = \begin{cases} q_l, & x < 0, \\ q_r, & x > 0. \end{cases} \tag{51}$$

For the linear advection equation 21, the solution to the Riemann problem consists of a discontinuity $q_r - q_l$ propagating at speed u along the characteristic (LeVeque, 2002). In the nonlinear case, the discontinuity or shock wave must propagate at speed s satisfying the Rankine-Hugonoit condition, given by

$$s = \frac{f(q_r) - f(q_l)}{q_r - q_l}. \tag{52}$$

The numerical flux $F_{i-1/2}^n$ at the cell interface located at $x = x_{i-1/2}$ can be obtained by solving the local Riemann problem with $q_l = Q_{i-1}^n$ and $q_r = Q_i^n$ and $x_{i-1/2}$ as the origin of the local coordinate system. The solution to the local Riemann problem at $x_{i-1/2}$ from time t_n to t_{n+1}, denoted as $Q_{i-1/2}^{\downarrow}$, will be a constant for any value of jump discontinuity $q_r - q_l$.

Godunov Scheme

The Godunov scheme can be written in the flux-differencing form given in equation 44 with the numerical flux

$$F_{i-1/2}^n = f(Q_{i-1/2}^{\downarrow}) \tag{53}$$

For the linear advection equation, the numerical flux can also be written in the form

$$F_{i-1/2}^n = u^+ Q_{i-1}^n + u^- Q_i^n, \tag{54}$$

where u^+ and u^- are defined as

$$\begin{aligned} u^+ &\equiv max(u,0) \\ u^- &\equiv min(u,0) \end{aligned} \tag{55}$$

The upwind scheme can be rewritten in the wave-propagating form as

$$Q_i^{n+1} = Q_i^n - \frac{\Delta t}{\Delta x}(u^+ W_{i-1/2} + u^- W_{i+1/2}), \tag{56}$$

where the wave $W_{i-1/2}$ is defined as

$$W_{i-1/2} \equiv \Delta Q_{i-1/2}^n = Q_i^n - Q_{i-1}^n. \tag{57}$$

The first-order upwind scheme is equivalent to the Godunov's method in this linear case and is first-order accurate in both time and space.

Lax-Wendroff Scheme

The Lax-Wendroff method is a second-order accurate, central scheme that uses the PDE to be solved to replace time derivatives in the Taylor's series expansion. To clarify this statement, I will use the linear advection equation $q_{,t} + uq_{,x} = 0$ as an example.

The Taylor's expansion of $q(x, t_{n+1})$ is given by

$$q(x,t_{n+1}) = q(x,t_n) + q_{,t}(x,t_n)\Delta t + q_{,tt}(x,t_n)\frac{(\Delta t)^2}{2!} + \cdots \tag{58}$$

Using the advection equation, the first time derivative in equation 58 is replaced by $q_{,t} = -uq_{,x}$, and differentiating this with respect to time gives

$$q_{,tt} = -uq_{,xt} = -u(q_{,t})_{,x} = u^2 q_{,xx} \tag{59}$$

Equation 58 then becomes

$$\begin{aligned} q(x,t_{n+1}) = \; & q(x,t_n) - uq_{,x}(x,t_n)\Delta t + u^2 q_{,xx}(x,t_n)\frac{(\Delta t)^2}{2!} \\ & + O((\Delta t)^3) \end{aligned} \tag{60}$$

Replacing the spatial derivatives in equation 60 by central finite difference approximations yields the Lax-Wendroff scheme

$$\begin{aligned} Q_i^{n+1} = \; & Q_i^n - \frac{1}{2}C(Q_{i+1}^n - Q_{i-1}^n) \\ & + \frac{1}{2}C^2(Q_{i+1}^n - 2Q_i^n + Q_{i-1}^n) \end{aligned} \tag{61}$$

where $C = u\Delta t/\Delta x$ is the Courant number.

The corresponding flux function for the Lax-Wendroff method is given by

$$F_{i-1/2}^n = \frac{1}{2}u(Q_{i-1}^n + Q_i^n) - \frac{1}{2}\frac{\Delta t}{\Delta x}u^2(Q_i^n - Q_{i-1}^n). \tag{62}$$

Beam-Warming Scheme

While the Lax-Wendroff scheme is centered and second-order accurate, the Beam-Warming scheme is also second-order accurate but one-sided, given by

$$\begin{aligned} Q_i^{n+1} = \; & Q_i^n - \frac{1}{2}C(3Q_i^n - 4Q_{i-1}^n + Q_{i-2}^n) \\ & + \frac{1}{2}C^2(Q_i^n - 2Q_{i-1}^n + Q_{i-2}^n) \end{aligned} \tag{63}$$

The corresponding flux function for the Beam-Warming method is given by

$$F_{i-1/2}^n = uQ_{i-1}^n + \frac{u}{2}(1-C)(Q_{i-1}^n - Q_{i-2}^n). \tag{64}$$

Fromm Scheme

The Fromm scheme is second-order accurate and non-symmetric, given by

$$\begin{aligned} Q_i^{n+1} = \; & Q_i^n - \frac{1}{4}C(Q_{i+1}^n + 3Q_i^n - 5Q_{i-1}^n + Q_{i-2}^n) \\ & + \frac{1}{4}C^2(Q_{i+1}^n - Q_i^n - Q_{i-1}^n + Q_{i-2}^n) \end{aligned} \tag{65}$$

Piecewise-Linear-Reconstruction Schemes

The Godunov's method uses the cell average Q_i^{n+1} to reconstruct the solution function $q(x, t_{n+1})$ as a piecewise constant function. This results in a first-order accurate method. To improve the accuracy, a piecewise linear reconstruction can be used instead by introducing a slope σ in each cell. The resulting method is second-order accurate. For the linear advection equation, the piecewise-linear-reconstruction (PLR) scheme can be written as

$$\begin{aligned} Q_i^{n+1} = \; & Q_i^n - C(Q_i^n - Q_{i-1}^n) \\ & - \frac{1}{2}C(\Delta x - u\Delta t)(\sigma_i^n - \sigma_{i-1}^n), \end{aligned} \tag{66}$$

where σ_i^n is the slope in the ith cell.

The Lax-Wendroff, Beam-Warming, and Fromm schemes can be obtained using the slopes defined below.

$$\begin{aligned} \text{Lax-Wendroff}: \;\; \sigma_i^n &= \frac{Q_{i+1}^n - Q_i^n}{\Delta x} \\ \text{Beam-Warming}: \;\; \sigma_i^n &= \frac{Q_i^n - Q_{i-1}^n}{\Delta x} \\ \text{Fromm}: \;\; \sigma_i^n &= \frac{Q_{i+1}^n - Q_{i-1}^n}{2\Delta x} \end{aligned} \tag{67}$$

Total Variation

These second-order schemes are more accurate than the Lax-Friedichs and Godunov methods but also introduce spurious oscillations where the solution is discontinuous. A mathematical way to measure the oscillation in a function is to use the total variation defined for grid function Q and differentiable function q as

$$TV(Q) \equiv \sum_{i=-\infty}^{\infty} |Q_i - Q_{i-1}| \tag{68}$$

$$TV(q) \equiv \int_{-\infty}^{\infty} |q'(x)| dx \tag{69}$$

TVD Schemes

A numerical scheme is called total variation diminishing (TVD) if it satisfies the inequality (LeVeque, 2002)

$$TV(Q^{n+1}) \le TV(Q^n) \tag{70}$$

From this definition, all the previously mentioned second-order schemes are not TVD. The next section introduces second-order TVD schemes.

Slope-Limiter Schemes

Monotonic Upstream-centered Scheme for Conservation Laws (MUSCL) is a class of numerical methods originally developed by van Leer (1979). The MUSCL scheme is the second-order extension of the first-order Godunov's method by applying a slope-limiter method to the piecewise linear reconstruction of the conserved variable q so that the monotonicity of the solution is preserved. This results in a second-order TVD scheme.

Here three slope-limiter methods presented in LeVeque (2002) are given as follows.

minmod limiter:

$$\sigma_i^n = \text{minmod}\left(\frac{Q_i^n - Q_{i-1}^n}{\Delta x}, \frac{Q_i^n - Q_{i-1}^n}{\Delta x}\right), \tag{71}$$

where the minmod function is defined as

$$\text{minmod}(a,b) = \begin{cases} a \text{ if } |a| < |b| \text{ and } ab > 0, \\ b \text{ if } |b| < |a| \text{ and } ab > 0, \\ 0 \text{ if } ab \le 0 \end{cases} \tag{72}$$

superbee limiter:

$$\sigma_i^n = \text{maxmod}(\sigma_i^{(1)}, \sigma_i^{(2)}), \tag{73}$$

where the maxmod function is defined as

$$\text{maxmod}(a,b) = \begin{cases} b \text{ if } |a| < |b| \text{ and } ab > 0, \\ a \text{ if } |b| < |a| \text{ and } ab > 0, \\ 0 \text{ if } ab \le 0 \end{cases} \tag{74}$$

and

$$\begin{aligned} \sigma_i^{(1)} &= \text{minmod}\left[\left(\frac{Q_{i+1}^n - Q_i^n}{\Delta x}\right), 2\left(\frac{Q_i^n - Q_{i-1}^n}{\Delta x}\right)\right], \\ \sigma_i^{(2)} &= \text{minmod}\left[2\left(\frac{Q_{i+1}^n - Q_i^n}{\Delta x}\right), \left(\frac{Q_i^n - Q_{i-1}^n}{\Delta x}\right)\right]. \end{aligned} \tag{75}$$

Monotonized central-difference (MC) limiter:

$$\sigma_i^n = \text{minmod}\left[\left(\frac{Q_{i+1}^n - Q_{i-1}^n}{2\Delta x}\right), 2\left(\frac{Q_i^n - Q_{i-1}^n}{\Delta x}\right), 2\left(\frac{Q_{i+1}^n - Q_i^n}{\Delta x}\right)\right] \tag{76}$$

Flux-Limiter Schemes

The piecewise-linear-reconstruction scheme can be rewritten into the flux-differencing form (equation 44) for the linear advection equation 21 with flux

$$F_{i-1/2}^n = u^- Q_i^n + u^+ Q_{i-1}^n + \frac{1}{2}|u|(1 - |C|)\delta_{i-1/2}^n, \tag{77}$$

where

$$\delta_{i-1/2}^n = \phi(\theta_{i-1/2}^n)\Delta Q_{i-1/2}^n. \tag{78}$$

Here $\theta_{i-1/2}^n$ is defined as

$$\theta_{i-1/2}^n \equiv \frac{\Delta Q_{I-1/2}^n}{\Delta Q_{i-1/2}^n} \tag{79}$$

where the index I is

$$I = \begin{cases} i-1 & \text{if } u > 0, \\ i+1 & \text{if } u < 0. \end{cases} \tag{80}$$

All the methods mentioned previously can be implemented as a flux-limiter method with the flux function $\phi(\theta)$ set as follows.

$$\begin{aligned} \text{Godunov}: &\ \phi(\theta) = 0, \\ \text{Lax-Wendroff}: &\ \phi(\theta) = 1, \\ \text{Beam-Warming}: &\ \phi(\theta) = \theta, \\ \text{Fromm}: &\ \phi(\theta) = \frac{1}{2}(1+\theta), \\ \text{minmod}: &\ \phi(\theta) = \text{minmod}(1,\theta), \\ \text{superbee}: &\ \phi(\theta) = \max(0, \min(1, 2\theta), \min(2, \theta)), \\ \text{MC}: &\ \phi(\theta) = \max(0, \min((1+\theta)/2, 2, 2\theta)). \end{aligned} \tag{81}$$

TVD Schemes for Nonlinear Problems

In nonlinear problems, a discontinuity in the initial data could lead to either a shock or rarefaction wave as shown in Figure 1. In most cases, the solution to the Riemann problem at $x_{i-1/2}$ denoted by $Q_{i-1/2}^{\downarrow}$ (the value of solution along the dotted line in Figure 1) will be either Q_{i-1} or Q_i. Only in the case of a centered rarefaction wave, $Q_{i-1/2}^{\downarrow}$ must be determined by the value q_s satisfying the conditions $Q_{i-1} < q_s < Q_i$ and $f'(q_s) = 0$; this is called the stagnation point or sonic point (LeVeque, 2002). In summary, $Q_{i-1/2}^{\downarrow}$ is given by

$$Q_{i-1/2}^{\downarrow} = \begin{cases} Q_{i-1} & \text{if } Q_{i-1} = Q_i \text{ or } s = 0, \\ Q_{i-1} & \text{if } Q_{i-1} > q_s \text{ and } s > 0, \\ Q_i & \text{if } Q_i < q_s \text{ and } s < 0, \\ q_s & \text{if } Q_{i-1} < q_s < Q_i, \end{cases} \tag{82}$$

where $s = (f(Q_i) - f(Q_{i-1}))/(Q_i - Q_{i-1})$ is the shock speed satisfying the Rankine-Hugonoit jump condition. Then, we can use the flux-differencing scheme in equation 44 with $F_{i-1/2}^n = f(Q_{i-1/2}^{\downarrow})$.

In addition to the flux-differencing form, the Godunov scheme can also be written in the fluctuation form given by

$$Q_i^{n+1} = Q_i^n - \frac{\Delta t}{\Delta x}(A^+ \Delta Q_{i-1/2}^n + A^- \Delta Q_{i+1/2}^n), \tag{83}$$

where the fluctuations $A^{\pm}\Delta Q_{i-1/2}^n$ are defined by

$$\begin{aligned} A^+ \Delta Q_{i-1/2}^n &\equiv f(Q_i) - f(Q_{i-1/2}^{\downarrow}), \\ A^- \Delta Q_{i-1/2}^n &\equiv f(Q_{i-1/2}^{\downarrow}) - f(Q_{i-1}^n. \end{aligned} \tag{84}$$

The Godunov scheme in the fluctuation form can be further extended to a high-resolution method by adding a correction term as (LeVeque, 2002)

$$Q_i^{n+1} = Q_i^n - \frac{\Delta t}{\Delta x}(A^+\Delta Q_{i-1/2}^n + A^-\Delta Q_{i+1/2}^n) - \frac{\Delta t}{\Delta x}(\tilde{F}_{i+1/2}^n - \tilde{F}_{i-1/2}^n), \tag{85}$$

where the corrected flux $\tilde{F}_{i-1/2}^n$ is defined by

$$\tilde{F}_{i-1/2}^n = \frac{1}{2}|s_{i-1/2}|\left(1 - \frac{\Delta t}{\Delta x}|s_{i-1/2}|\right)\delta_{i-1/2}^n, \tag{86}$$

and the speed $s_{i-1/2}$ is defined by

$$s_{i-1/2} = \begin{cases} (f(Q_i) - f(Q_{i-1}))/(Q_i - Q_{i-1}) & \text{if } Q_{i-1} \neq Q_i, \\ f'(Q_i) & \text{if } Q_{i-1} = Q_i. \end{cases} \tag{87}$$

Godunov Method for Linear Systems

Given a linear system

$$q_{,t} + Aq_{,x} = 0, \tag{88}$$

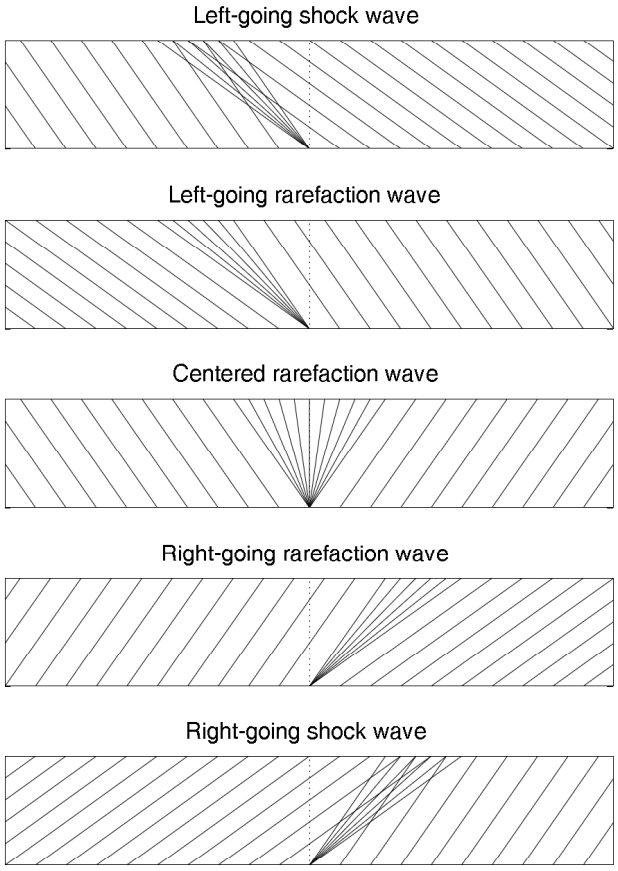

Figure 1: Patterns of characteristics corresponding to 5 initial piecewise-constant data with a jump discontinuity for the Burgers equation.

where q is an m-vector of conserved quantities and A is a constant coefficient matrix. If the system is hyperbolic, all the eigenvalues of A must be real and the system can be diagonalized by the similarity transformation

$$R^{-1}AR = \Lambda, \tag{89}$$

where R is the matrix whose columns are the right eigenvectors r_p, $p = 1, 2, ..., m$. If all the eigenvectors r_p are unit vector, R will be a diagonal matrix, i.e., $RR^T = R^TR = I$, where I is the identity matrix. By introducing the characteristic variable $w = R^{-1}q$, we obtain the diagonalized system

$$w_{,t} + \Lambda w_{,x} = 0, \tag{90}$$

which corresponds to m decoupled linear advection equations.

The Godunov method can be implemented for the linear system using the fluctuation form (equation 83) with A^+ and A^- defined by

$$A^+ = R\Lambda^+R^{-1}, \quad A^- = R\Lambda^-R^{-1}, \tag{91}$$

where

$$\Lambda^+ = \text{diagonal}(\lambda_p^+), \quad \Lambda^- = \text{diagonal}(\lambda_p^-). \tag{92}$$

Here λ_p^+ and λ_p^- are defined as

$$\lambda_p^+ \equiv \max(\lambda_p, 0), \quad \lambda_p^- \equiv \min(\lambda_p, 0). \tag{93}$$

High-Resolution Methods for Linear Systems

The correct flux $\tilde{F}_{i-1/2}^n$ for linear systems is

$$\tilde{F}_{i-1/2}^n = \frac{1}{2}|A|\left(1 - \frac{\Delta t}{\Delta x}|A|\right)\sum_{p=1}^m \tilde{\alpha}_{i-1/2}^p r^p, \tag{94}$$

where $|A| = A_+ - A^-$ and r^p is the p-th right eigenvector of A. Here $\tilde{\alpha}_{i-1/2}^p$ is the limited version of $\alpha_{i-1/2}^p = R^{-1}\Delta Q_{i-1/2}^n$, given by

$$\tilde{\alpha}_{i-1/2}^p = \alpha_{i-1/2}^p \phi(\theta_{i-1/2}^p), \tag{95}$$

where ϕ is one of the limiter functions given previously,

$$\theta_{i-1/2}^p = \frac{\alpha_{I-1/2}^p}{\alpha_{i-1/2}^p} \tag{96}$$

and the index I is

$$I = \begin{cases} i-1 & \text{if } \lambda^p > 0, \\ i+1 & \text{if } \lambda^p < 0. \end{cases} \tag{97}$$

Since $|A|r^p = |\lambda^p|r^p$, the corrected flux $\tilde{F}_{i-1/2}^p$ can also be written as

$$\tilde{F}_{i-1/2}^n = \frac{1}{2}\sum_{p=1}^m |\lambda^p|\left(1 - \frac{\Delta t}{\Delta x}|\lambda^p|\right)\tilde{\alpha}_{i-1/2}^p r^p. \tag{98}$$

Numerical Results

Linear Advection Equation

In this section, I apply the numerical schemes presented earlier to numerically solve the linear advection equation. The numerical calculations were performed in the domain $[0, 1]$ with the grid spacing $\Delta x = 0.01$ m, the Courant number $C = u\Delta t/\Delta x = 0.8$, the flow velocity $u = 1$ m/s, the time limit $T = 5$ s, and the initial condition

$$q(x,0) = \begin{cases} 1, & 0.6 \le x \le 0.8, \\ e^{-200(x-0.3)^2}, & \text{otherwise.} \end{cases} \tag{99}$$

The numerical results at the time limit shown in Figure 2 show the strong numerical dissipation property of the Lax-Friedichs and Godunov methods which are first-order accurate. There are small-amplitude oscillations in the Lax-Friedichs solution. Since the Godunov's method is TVD, its solution has no spurious oscillation. Among the second-order non-TVD methods, the Fromm method provides the most accurate result with small oscillation compared to that of the Lax-Wendroff and Beam-Warming methods. Among the second-order TVD methods, the MUSCL scheme with superbee limiter provides the most accurate result in both the smooth and discontinous regions.

Burgers Equation

In this section I applied the numerical schemes to solve the Burgers equation in various cases.

Rarefaction wave only: In the first case, the calculations were performed in the domain $[0, 1]$ with the grid spacing $\Delta x = 0.04$ m, the time sampling interval $\Delta t = 0.032$ s, the time limit $T = 0.3$ s, and the initial condition is

$$u(x,0) = \begin{cases} -1 & \text{if } x < 0.5, \\ 1 & \text{if } x > 0.5. \end{cases} \tag{100}$$

This initial condition will lead to a centered rarefaction wave propagating in both directions. The numerical results shown in Figure 3 show that, among the first-order methods, the Godunov method provides a more accurate result than the Lax-Friedichs method. For an explanation on the staircase pattern of the Lax-Friedichs method, see section 12.5 of LeVeque (2002). For the second-order methods, all methods provide comparably accurate results.

Shock wave only: In the second case, the calculations were performed in the domain $[0, 1]$ with the grid spacing $\Delta x = 0.01$ m, the time sampling interval $\Delta t = 0.008$ s, the time limit $T = 0.3$ s, and the initial condition is

$$u(x,0) = \begin{cases} 1 & \text{if } x < 0.5, \\ 0.1 & \text{if } x > 0.5. \end{cases} \tag{101}$$

This initial condition will lead to a shock wave propagating to the right with speed $s = 1.05$. The numerical results shown in Figure 4 show that all TVD methods and the Lax-Wendroff method can accurately capture the shock wave. However, the Lax-Wendroff method also gives rise to an upshoot at the discontinuity. In the case of the

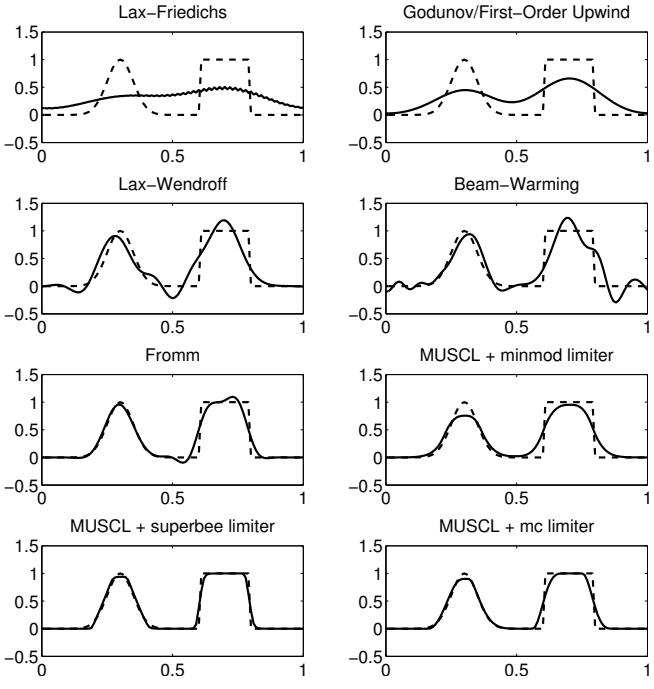

Figure 2: Numerical results to the linear advection equation using various methods. The dashed and solid lines represent the exact and numerical solutions, respectively.

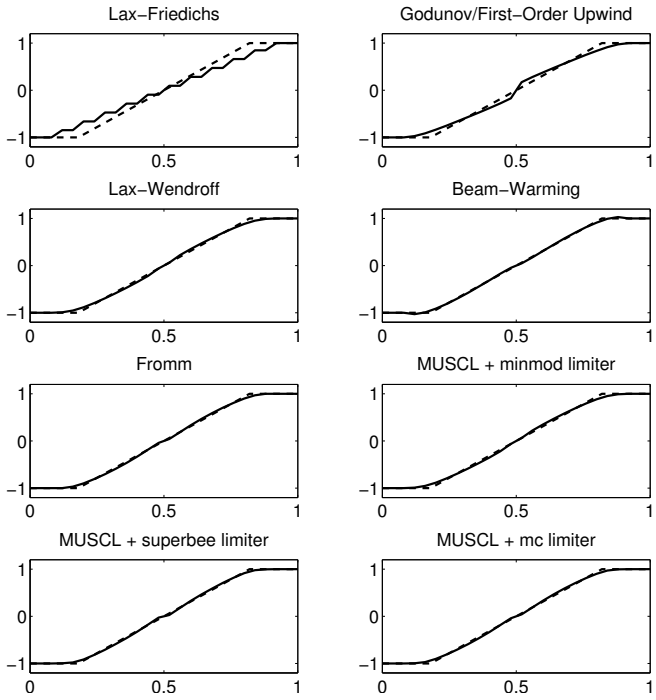

Figure 3: Numerical results to the Burgers equation in the case of a rarefaction wave only. The dashed and solid lines represent the exact and numerical solutions, respectively.

Beam-Warming and Fromm methods, there is an instability initiating from the discontinuity and propagating away in both directions so the result is missing in this region.

Shock and rarefaction waves: In the third case, the calculations were performed in the domain $[0, 1]$ with the grid spacing $\Delta x = 0.01$ m, the time sampling interval $\Delta t = 0.008$ s, the time limit $T = 0.5$ s, and the initial condition is

$$u(x, 0) = e^{-200(x-0.3)^2}. \tag{102}$$

According to the numerical results shown in Figure 5, only the Lax-Wendroff and Fromm methods provide solution with spurious oscillations while the Beam-Warming scheme provide a sharp result at the shock wave front even though it is not TVD. The Beam-Warming result is comparable to that of the MUSCL schemes. The Godunov method provides a slightly smooth result compared to that of the MUSCL schemes. The Lax-Friedichs method provides the smoothest result.

Acoustics Equations

In this section I applied the numerical schemes to solve the acoustics equations. The calculations were performed in the domain $[0, 1]$ with the grid spacing $\Delta x = 0.002$ m, the bulk modulus $K_0 = 0.1$, the density $\rho_0 = 1$, the fluid velocity $u_0 = 0$, the time sampling interval $\Delta t = 0.0032$ s, the time limit $T = 1$ s, and the initial conditions are

$$p(x, 0) = \begin{cases} 1 & \text{if } 0.5 < x < 0.6, \\ e^{-400(x-0.4)^2} & \text{otherwise,} \end{cases} \tag{103}$$
$$u(x, 0) = 0.$$

The numerical results shown in Figure 6 only include the results of the Godunov scheme, Lax-Wendroff scheme, and MUSCL schemes with midmod and superbee limiters. The Lax-Friedichs scheme gave quite an inaccurate result and so its result is not included. The Beam-Warming and Fromm schemes are unstable in this case. According to the results shown in Figure 6, the Godunov scheme provides a slightly smooth result compared to the other second-order methods.

1D Shallow-Water Equations

In this section I applied the numerical schemes to solve the 1D shallow-water equations. The calculations were performed in the domain $[-5, 5]$ with the grid spacing $\Delta x = 0.002$ m, the time sampling interval $\Delta t = 0.5\Delta x / \max(v(x, 0))$ where the gravitational wave speed $v(x, 0) = \sqrt{gh(x, 0)}$, the gravitational acceleration $g = 1$ m/s^2, the time limit $T = 3$ s, and the initial conditions for the wave height h and fluid particle velocity u are

$$\begin{aligned} h(x, 0) &= 1 + 0.4e^{-5x^2}, \\ u(x, 0) &= 0. \end{aligned} \tag{104}$$

In this case, the initial wave height contains a large-amplitude Gaussian hump which then later becomes shock waves propagating in both directions as shown in Figure 7. I only

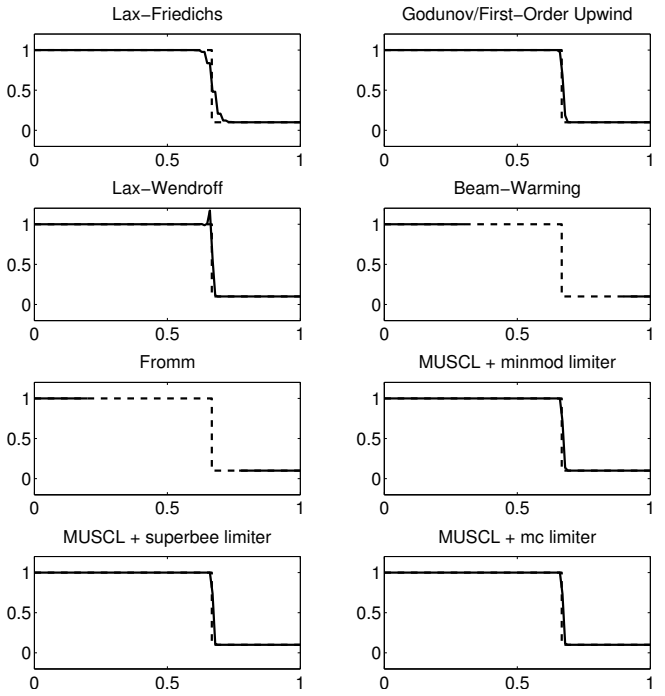

Figure 4: Numerical results to the Burgers equation in the case of a shock wave only. The dashed and solid lines represent the exact and numerical solutions, respectively.

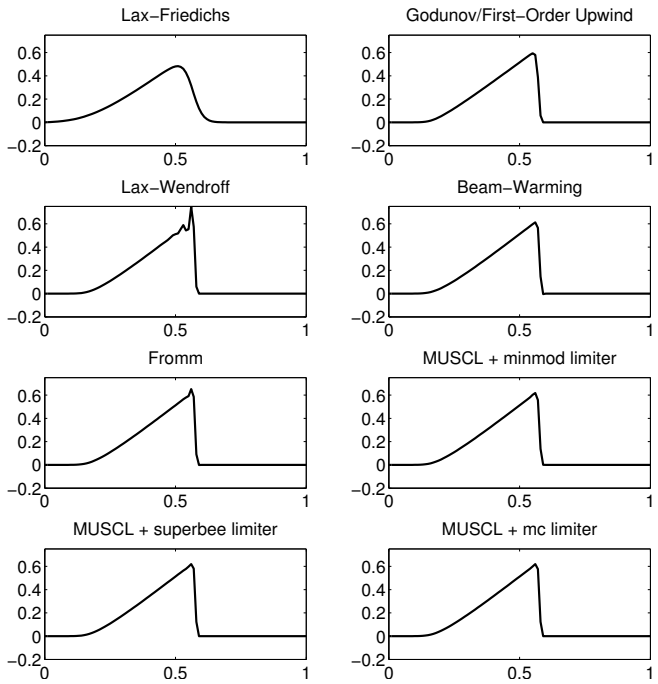

Figure 5: Numerical results to the Burgers equation in the case of shock and rarefaction waves.

applied some methods to this problem including the Godunov scheme, the Lax-Wendroff scheme, and the MUSCL schemes with minmod, superbee, and MC limiters. The Lax-Wendroff scheme provides a result with spurious oscillations at the shock wave fronts. All MUSCL schemes provide comparable results so only the results from minmod and superbee limiters are shown. The Godunov method provides a slightly smooth result at the shock wave fronts compared to the MUSCL schemes.

SUMMARY

In this report, I present a new PML formulation for the shallow-water equations and the theory of finite volume method. Due to the lack of a stable PML formulation for the nonlinear shallow-water equations, the proposed PML formulation could, hopefully, lead to a new research finding and, consequently, a publication. Using the finite volume method, I will numerically solve the proposed PML formulation in the next six-month period to assess its effectiveness and stability. In the section of finite volume method, I also present the numerical results obtained from solving various problems using the finite-volume methods presented in this report. The results show that the MUSCL schemes are very effective for solving problems containing discontinuitites in the form of shock and/or rarefaction waves.

REFERENCES

Abarbanel, S. and D. Gottleib, 1997, A mathematical analysis of the pml method: Journal of Computational Physics, **134**, 357–363.

———, 1998, On the construction and analysis of absorbing layers in cem: Applied Numerical Mathematics, **27**, 331–340.

Abarbanel, S., D. Gottleib, and J. S. Hesthaven, 1999, Well-posed perfectly matched layers for advective acoustics: Journal of Computational Physics, **154**, 266–283.

Abarbanel, S., D. Stanescu, and M. Y. Hussaini, 2003, Unsplit variables perfectly matched layers for the shallow water equations with coriolis forces: Computational Geosciences, **7**, 275–294.

Barucq, H., J. Diaz, and M. Tlemcani, 2010, New absorbing layers conditions for short water waves: Journal of Computational Physics, **229**, 58–72.

Bérenger, J. P., 1994, A perfectly matched layer for the absorption of electromagnetic waves: Journal of Computational Physics, **114**, 185–200.

Chew, W. C. and W. H. Weedon, 1994, A 3d perfectly matched medium from modified maxwell's equations with stretched coordinates: Microwave and Optical Technology Letters, **7**, 599–604.

Hesthaven, J. S., 1998, On the analysis and construction of perfectly matched layers for the linearized euler equations: Journal of Computational Physics, **142**, 129–147.

Hu, F. Q., 1996, On absorbing boundary conditions for linearized euler equations by a perfectly matched layer: Journal of Computational Physics, **129**, 201–219.

———, 2001, A stable, perfectly matched layer for linearized euler equations in unsplit physical variables: Journal of Computational Physics, **173**, 455–480.

LeVeque, R. J., 2002, Finite volume methods for hyper-

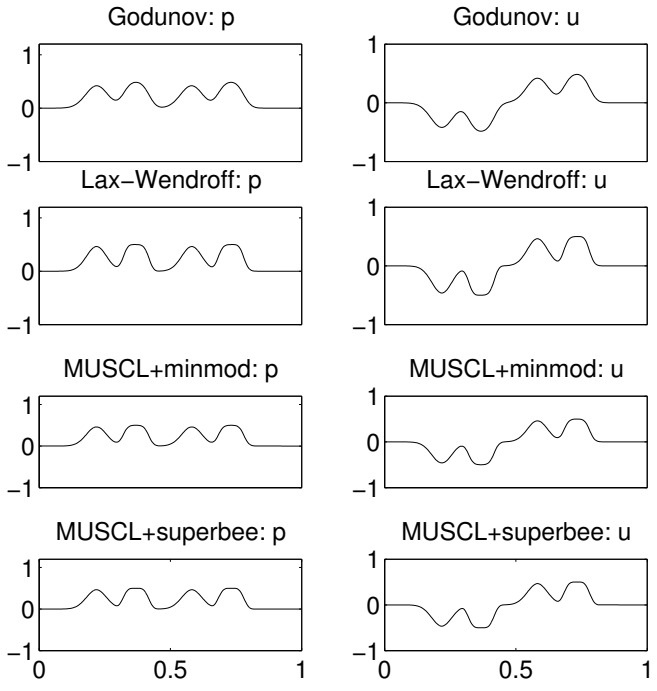

Figure 6: Numerical results to the acoustics equations.

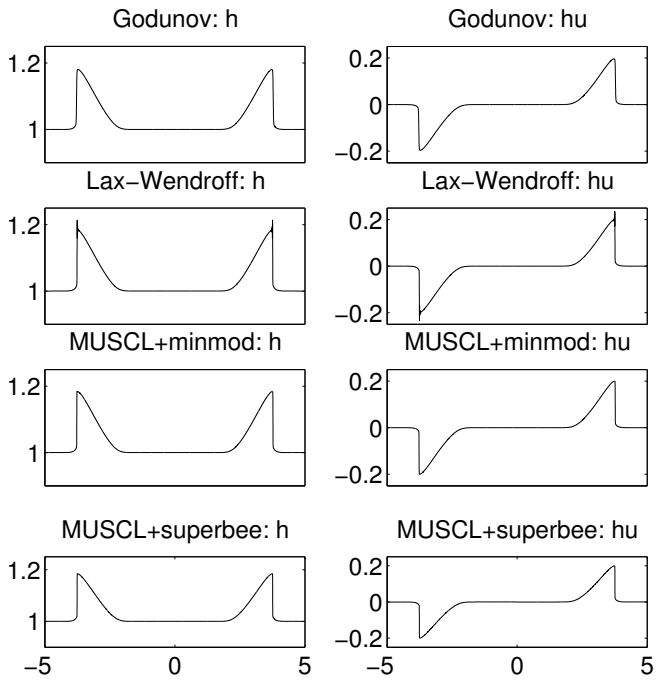

Figure 7: Numerical results to the 1D shallow-water equations.

bolic problems: Cambridge University Press.

Nataf, F., 2006, A new approach to perfectly matched layers for the linearized euler system: Journal of Computational Physics, **214**, 757–772.

Navon, I. M., B. Neta, and M. Y. Hussaini, 2004, A perfectly matched layer approach to the linearized shallow water equations models: Monthly Weather Review, **132**, 1369–1378.

van Leer, B., 1979, Towards the ultimate conservative difference scheme v. a second order sequel to godunov's method: Journal of Computational Physics, **32**, 101–136.